Available online at www.sciencedirect.com
ScienceDirect
Journal of Power Sources 179 (2008) 566–570
JOURNAL OF POWER SOURCES
www.elsevier.com/locate/jpowsour

Short communication

Hydrogen production via steam reforming of ethyl alcohol over nano-structured indium oxide catalysts

Tetsuo Umegaki, Kentaro Kuratani, Yusuke Yamada, Atsushi Ueda, Nobuhiro Kuriyama, Tetsuhiko Kobayashi, Qiang Xu *

National Institute of Advanced Industrial Science and Technology (AIST), 1-8-31 Midorigaoka, Ikeda, Osaka 563-8577, Japan

Received 28 August 2007; received in revised form 5 January 2008; accepted 8 January 2008
Available online 16 January 2008

Abstract

Mesoporous and worm-like In_2O_3 catalysts have been prepared using KIT-6 and MCM-41 silicas as templates, which show low crystallinities and high surface areas. Compared with commercial In_2O_3 catalyst with low surface area, these two nano-structured In_2O_3 catalysts exhibit higher catalytic activity for steam reforming of ethyl alcohol at low temperature to produce hydrogen containing no detectable CO impurity, presenting an advantage in comparison with the previous reported catalysts.

Keywords: In_2O_3 catalysts; Nano-structured; Silica templates; Hydrogen production; Ethyl alcohol

1. Introduction

Recently, significant progress has been achieved in the preparation of nano-structured materials by utilizing the so-called *nano-casting* route [1,2]. According to this method, an ordered porous carbon or silica matrix acts as nano-scopic mold, which restricts, through confinement, the formation and growth of metal or metal oxide species [3–6]. Various nano-objects such as nano-particles, nano-wires, or nano-structured networks can form selectively in the voids of porous silica, and have potential applications such as catalysts [7–9], new materials for gas sensors [10,11], and precursors of anode materials in Li-ion rechargeable batteries [10,12] because of their large specific surface areas and shape-selective properties, which enhance the efficiency of catalysis, conduction, and adsorption.

Ethyl alcohol is preferable as the hydrogen resources for the fuel cells compared with other resources since it can be easily produced from biomass by fermentation [13]. The most effective process for hydrogen production from ethyl alcohol is the steam reforming reaction, $C_2H_5OH + 3H_2O \rightarrow 2CO_2 + 6H_2$. For this reaction, Co- [14–17], Ni- [18–21], or Rh- [22,23] based catalysts exhibited high activities, whereas a high reaction temperature (>623 K) is required to obtain high hydrogen yield, and CO is generated as by-product, which should be removed to prevent from the poisoning of electrode catalysts of fuel cells. On the other hand, there have been limited examples of indium catalysts thus far; only some composite catalysts including indium as a promoter or co-catalyst have been reported [24–26]. Here we report the first high performance single-component indium oxide catalysts for the steam reforming of ethyl alcohol, which produces hydrogen with low CO concentration at low temperature.

2. Experimental

2.1. Catalyst preparation

Commercial and prepared In_2O_3 catalysts were used for the steam reforming of ethyl alcohol. The commercial In_2O_3 catalyst was purchased from Mitsuwa Chem. Co. Two nano-structured In_2O_3 catalysts were prepared with mesoporous KIT-6 [27,28] and MCM-41 [29,30] silicas as templates. The KIT-6 template was prepared according to the reported procedure [27,28], while MCM-41 was commercially purchased (Aldrich Chem. Co.). The templates were immersed in 0.1 M aqueous solution of indium nitrate (Kishida Chem. Co.) for 2 h.

* Corresponding author. Tel.: +81 72 751 9562; fax: +81 72 751 9629.
E-mail address: q.xu@aist.go.jp (Q. Xu).

0378-7753/$ – see front matter © 2008 Elsevier B.V. All rights reserved.
doi:10.1016/j.jpowsour.2008.01.010

After drying at 393 K, the samples were calcined in air at 623 K for 3 h. Nano-structured In_2O_3 materials were obtained through the solution etching of silica framework by a 1.0 M NaOH aqueous solution. The resulting materials were then centrifugally separated, washed with distilled water to pH 7, and dried at 383 K.

2.2. Characterization of catalysts

Powder XRD measurements were performed on a RINT2200 diffractometer (Rigaku) equipped with a Cu Kα X-ray tube operating at 40 kV and 40 mA at a scanning rate of $0.02^\circ\ s^{-1}$. Transmission electron microscopy (TEM) measurements were carried out on a H-9000NA equipment (Hitachi). Specific surface areas of the In_2O_3 catalysts were determined by N_2 adsorption on a Quantasorb Jr equipment (Quantachrome Co.). The catalysts were outgassed at 473 K prior to N_2 adsorption. The surface areas were calculated by the BET method using the N_2 adsorption isotherm at 77 K. X-ray photoelectron spectra (XPS) were acquired with an ESCA-3400 spectrometer (Simadzu) equipped with a Mg Kα X-ray exciting source (1253.6 eV) operating at 10 kV and 10 mA. The binding energies (BE) were referred to the C 1s peak at 284.9 eV.

2.3. Evaluation of catalytic performance

The In_2O_3 catalysts (65 mg) held in L-shaped quartz tubes were loaded in a fixed-bed flow reactor (TPR-5D, Bell Japan Inc.). The catalytic activity measurements were performed with an electrically heated reactor equipped with a thermocouple that allowed temperature measurement inside the catalytic bed. A flow of 0.4% C_2H_5OH/1.6% H_2O in N_2 stream (molar ratio) was introduced into the reactor with a rate of 50 mL min^{-1} at 498, 523, 548, 573, and 623 K. The C_2H_5OH–H_2O liquid mixture was supplied by a syringe pump (KD Science) and vaporized at 403 K, and then mixed with the N_2 flow and introduced into the reactor. Effluent gas was analyzed by two on-line microgas chromatographs, GC3000A and M-200H (Agilent), equipped with TC detectors for 10 h at each reaction temperature. An induction time was first observed for each catalyst and then the catalytic activity was kept constant. GC3000A is equipped with Porapak Q for separating CO_2, C_2H_4, C_2H_6, C_3H_6, CH_3CHO, and C_2H_5OH, and Molecular Sieve 5A for separating H_2, CO, and CH_4. M-200H is equipped with Porapak Q for separating C_2H_4, C_2H_6, C_3H_6, CH_3CHO, C_2H_5OH, and CH_3COCH_3, and Molecular Sieve 5A for separating CO and CH_4. The detection limit of CO is <50 ppm.

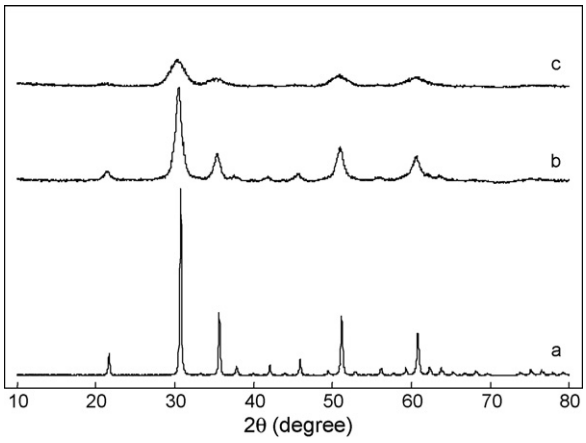

Fig. 1. XRD profiles of (a) commercial, (b) mesoporous (KIT-6), and (c) worm-like (MCM-41) In_2O_3 catalysts.

3. Results and discussion

3.1. Catalyst characterization

Fig. 1 shows XRD profiles of the commercial and prepared In_2O_3 catalysts. The commercial In_2O_3 catalyst shows sharp peaks, whereas the nano-structured In_2O_3 catalysts prepared with the KIT-6 and MCM-41 silica templates exhibit broadened diffraction peaks at the same positions, indicating that the commercial In_2O_3 catalyst has high crystallinity and the prepared nano-structured In_2O_3 catalysts have lower crystallinities.

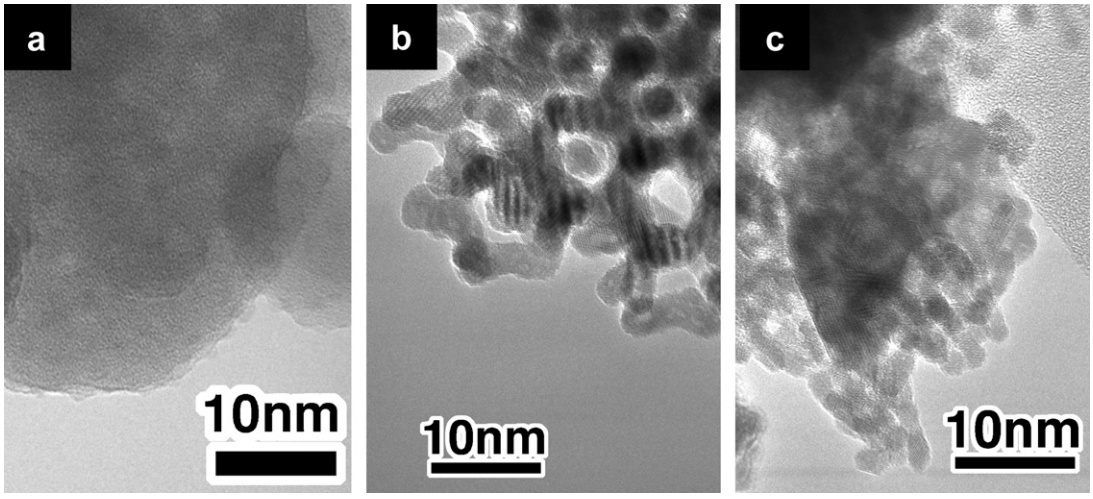

Fig. 2. TEM images of (a) commercial, (b) mesoporous (KIT-6), and (c) worm-like (MCM-41) In_2O_3 catalysts.

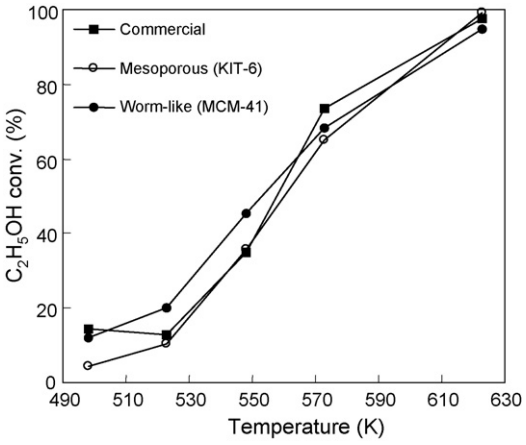

Fig. 3. Ethyl alcohol conversion over In_2O_3 catalysts. Reaction conditions: $C_2H_5OH:H_2O:N_2 = 0.4:1.6:98$ (molar ratio), $N_2 = 50\,mL\,min^{-1}$, time on stream = 10 h.

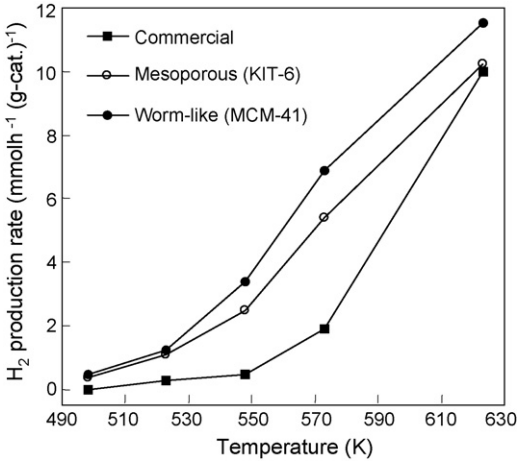

Fig. 4. Hydrogen production rate over In_2O_3 catalysts. Reaction conditions: $C_2H_5OH:H_2O:N_2 = 0.4:1.6:98$ (molar ratio), $N_2 = 50\,mL\,min^{-1}$, time on stream = 10 h.

Fig. 2 shows TEM images of the commercial and prepared nano-structured In_2O_3 catalysts. In comparison with the commercial one (Fig. 2a), a mesoporous structure was observed for the In_2O_3 catalyst prepared using the KIT-6 template, which has a 3D mesopore structure; the pore diameter (7.5 nm) of the mesoporous In_2O_3 corresponds to the wall thickness of the KIT-6 template and the wall thickness (2.0–3.0 nm) of In_2O_3 corresponds to the pore diameter of the KIT-6 template. On the other hand, not a mesoporous but worm-like structure was observed for the In_2O_3 catalyst prepared using the MCM-41 template, reflecting the 1D channel structure for the template [29,30]. The diameter of worm-like In_2O_3 catalyst (2.5 nm) corresponds to the 1D pore diameter of the MCM-41 template (3.4–4.0 nm) [30]. BET measurement reveals that the commercial In_2O_3 catalyst with a high crystallinity has a surface area of $7\,m^2\,g^{-1}$. The mesoporous In_2O_3 catalyst has higher surface area ($107\,m^2\,g^{-1}$) and the worm-like In_2O_3 catalyst has the highest value ($173\,m^2\,g^{-1}$), in agreement with their low crystallinities as observed by powder XRD measurements.

3.2. Catalyst activity

All the catalysts show conversions of ethyl alcohol at the same levels at each temperature (Fig. 3). In comparison with the commercial In_2O_3 catalyst, the mesoporous In_2O_3 catalyst gives higher hydrogen production rates at all the temperatures (Fig. 4). The worm-like In_2O_3 catalyst prepared with the MCM-41 template shows the highest hydrogen production rates at all the temperatures. The product distribution reflects the differences in the catalytically active sites on the surfaces of the catalysts with different structures. Table 1 shows the product selectivities over the In_2O_3 catalysts at 498–623 K. The commercial In_2O_3 catalyst mainly affords the dehydrate product C_2H_4 at

Table 1
Product distributions over In_2O_3 catalysts

Catalysts	T(K)	Conversion (%)	Selectivity (%)[a]					
			H_2	CO_2	C_2H_4	C_3H_6	CH_3CHO	CH_3COCH_3
Commercial	498	14.8	–	–	93.4	–	6.6	–
	523	12.7	14.3	–	76.2	–	9.5	–
	548	35.1	19.6	–	68.4	–	11.9	–
	573	73.6	26.4	4.3	54.2	0.8	7.0	7.2
	623	97.8	57.1	13.7	6.6	0.5	0.8	21.2
Mesoporous (KIT-6)	498	4.2	54.3	–	–	–	45.7	–
	523	10.6	53.1	–	–	–	46.9	–
	548	35.7	56.1	–	0.9	1.4	41.6	–
	573	65.2	54.8	2.8	1.7	1.7	33.2	5.8
	623	99.2	58.8	16.8	0.4	2.0	1.5	20.4
Worm-like (MCM-41)	498	12.0	58.1	–	–	–	41.9	–
	523	19.9	58.5	–	–	2.8	38.8	–
	548	45.5	61.5	–	–	2.2	30.5	5.8
	573	68.2	59.0	6.7	0.7	1.9	20.2	11.4
	623	94.6	64.0	13.0	0.1	1.3	6.0	15.6

Reaction conditions: $C_2H_5OH:H_2O:N_2 = 0.4:1.6:98$ (molar ratio), $N_2 = 50\,mL\,min^{-1}$, time on stream = 10 h.
[a] Molar percentage of products.

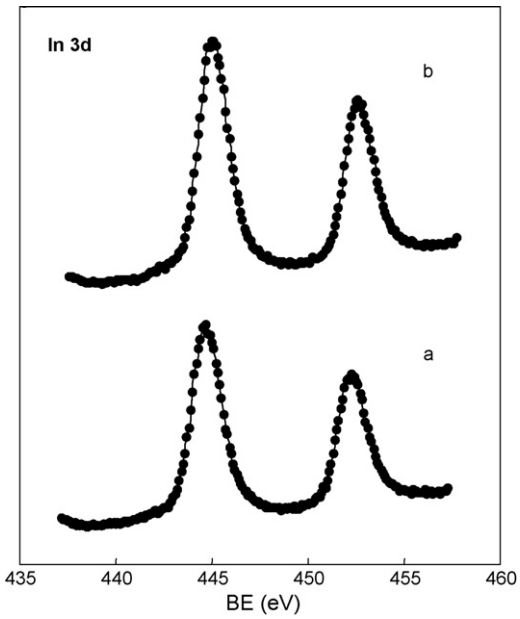

Fig. 5. X-ray photoelectron spectra in the In 3d region for the worm-like In_2O_3 catalysts (a) before and (b) after reaction at 573 K.

low temperatures (Eq (1))

$$C_2H_5OH \rightarrow C_2H_4 + H_2O \quad (1)$$

It is noted that ethyl alcohol is converted without hydrogen production via this reaction route and dehydration is the undesirable path for hydrogen production. In contrast, the mesoporous (KIT-6) and the worm-like (MCM-41) In_2O_3 catalysts mainly afford the products H_2, CH_3CHO and CH_3COCH_3. It is proposed that CH_3CHO is generated by the dehydrogenation of ethyl alcohol (Eq. (2)) [31]. The CH_3CHO may be further converted to CH_3COCH_3 via aldol condensation with hydrogen production (Eq. (3)) [31].

$$C_2H_5OH \rightarrow CH_3CHO + H_2 \quad (2)$$

$$2CH_3CHO + H_2O \rightarrow CO_2 + CH_3COCH_3 + 2H_2 \quad (3)$$

It is noted that hydrogen is produced in reaction (2) and (3). The reaction (3) was also observed over CuO/CeO_2 [31], Fe_2O_3/ZnO [32], and ZnO/CaO [33,34].

Fig. 5 shows the In 3d XPS spectra of worm-like In_2O_3 catalysts before and after reaction at 573 K. The characteristic spin–orbit split $3d_{5/2}$ and $3d_{3/2}$ signals are attributed to In_2O_3 [35–37]. No marked differences were observed for the samples before and after the reaction, suggesting that In_2O_3 is the active phase for the reforming reaction of ethyl alcohol. In addition, peak areas of the C 1s XPS spectra of worm-like In_2O_3 catalysts keep unchanged before and after the reaction, suggesting negligible amount of coke formation on the worm-like In_2O_3 catalyst.

Over the present In_2O_3 catalysts, no CO impurity was detected within the detection limit (<50 ppm). In contrast, it was previously reported that Co-, Ni-, and Rh-based catalysts yield high concentration CO by-product up to 8%. It was suggested that the reverse water-gas shift reaction of CO_2 and H_2, the products of the steam reforming of ethyl alcohol, produces CO as by-product on the Co, Ni, and Ir/CeO_2 catalysts (Eq. (4)) [38].

$$CO_2 + H_2 \rightarrow CO + H_2O \quad (4)$$

The absence of CO in the present experiments may be due to the low activity of the In_2O_3 catalysts for the reverse water-gas shift reaction.

4. Conclusions

Mesoporous and worm-like In_2O_3 catalysts have been prepared using KIT-6 and MCM-41 silicas as templates, which have low crystallinities and high surface areas. These two nanostructured In_2O_3 catalysts exhibit high hydrogen production rate from ethyl alcohol at low temperatures. The In_2O_3 catalysts yield low-concentration CO impurity, presenting an advantage in comparison with previous reported catalysts.

References

[1] F. Schüth, Angew. Chem. Int. Ed. 42 (2003) 3604–3622.
[2] H. Yang, D. Zhao, J. Mater. Chem. 15 (2005) 1217–1231.
[3] H.J. Shin, C.H. Ko, R. Ryoo, J. Mater. Chem. 11 (2001) 260–261.
[4] B. Tian, X. Liu, H. Yang, S. Xie, C. Yu, B. Tu, D. Zhao, Adv. Mater. 15 (2003) 1370–1374.
[5] B. Tian, X. Liu, L.A. Solovyov, Z. Liu, H. Yang, Z. Zhang, S. Xie, F. Zhang, B. Tu, C. Yu, O. Terasaki, D. Zhao, J. Am. Chem. Soc. 126 (2004) 865–875.
[6] Y. Wang, C.-M. Yang, W. Schmidt, B. Spliethoff, E. Bill, F. Schüth, Adv. Mater. 17 (2005) 53–56.
[7] L. Yan, X. Zhang, T. Ren, H. Zhang, X. Wang, J. Suo, Chem. Commun. (2002) 860–861.
[8] R. Moreno-Tost, J. Santamaría-González, P. Maireles-Torres, E. Rodríguez-Castellón, A. Jiménez-López, J. Mater. Chem. 12 (2002) 3331–3336.
[9] J.W. Miao, J. Zhou, G.H. Song, Y.N. Fan, C. Gong, Chin. J. Inorg. Chem. 21 (2005) 1541–1545.
[10] W.-Y. Li, L.-N. Xu, J. Chen, Adv. Funct. Mater. 15 (2005) 851–857.
[11] I. Hotovy, V. Rehacek, P. Siciliano, S. Capone, L. Spiess, Thin Solid Films 418 (2002) 9–15.
[12] F. Jiao, K.M. Shaju, P.G. Bruce, Angew. Chem. Int. Ed. 44 (2005) 6550–6553.
[13] G.A. Deluga, J.R. Salge, L.D. Schmidt, X.E. Verykios, Science 303 (2004) 993–997.
[14] F. Haga, T. Nakajima, H. Miya, S. Mishima, Catal. Lett. 48 (1997) 223–227.
[15] J. Llorca, P. Ramírez de la Piscina, J.-A. Dalmon, J. Sales, N. Homs, Appl. Catal. B: Environ. 43 (2003) 355–369.
[16] J. Llorca, N. Homs, P. Ramírez de la Piscina, J. Catal. 227 (2004) 556–560.
[17] V.A. de la Peña O' Shea, N. Homs, E.B. Pereira, R. Nafria, P. Ramírez de la Piscina, Catal. Today 126 (2007) 148–152.
[18] A.N. Fatsikostas, D.I. Kondarides, X.E. Verykios, Chem. Commun. (2001) 851–852.
[19] A.N. Fatsikostas, X.E. Verykios, J. Catal. 225 (2004) 439–452.
[20] V.S. Bergamaschi, F.M.S. Carvalho, C. Rodrigues, D.B. Fernandes, Chem. Eng. J. 112 (2005) 153–158.
[21] M.C. Sánchez-Sánchez, R.M. Navarro, J.L.G. Fierro, Int. J. Hydrogen Energy 32 (2007) 1462–1471.
[22] C. Diagne, H. Idriss, A. Kiennemann, Catal. Commun. 3 (2002) 565–571.
[23] J. Raskó, A. Hancz, A. Erdőhelyi, Appl. Catal. A: Gen. 269 (2004) 13–25.
[24] M. Ogura, E. Kikuchi, Chem. Lett. (1996) 1017–1018.
[25] M. Haneda, Y. Kintaichi, H. Hamada, Catal. Lett. 55 (1998) 47–55.
[26] V. Pârvulescu, S. Coman, V.I. Pârvulescu, P. Grange, G. Poncelet, J. Catal. 180 (1998) 66–84.
[27] F. Kleitz, S.H. Choi, R. Ryoo, Chem. Commun. (2003) 2136–2137.

[28] T.-W. Kim, F. Kleitz, B. Paul, R. Ryoo, J. Am. Chem. Soc. 127 (2005) 7601–7610.
[29] J.S. Beck, J.C. Vartuli, W.J. Roth, M.E. Leonowicz, C.T. Kresge, K.D. Schmitt, C.T-W. Chu, D.H. Olson, E.W. Sheppard, S.B. McCullen, J.B. Higgins, J.L. Schlenker, J. Am. Chem. Soc. 114 (1992) 10834–10843.
[30] T.R. Pauly, V. Petkov, Y. Liu, S.J.L. Billinge, T.J. Pinnavaia, J. Am. Chem. Soc. 124 (2002) 97–103.
[31] T. Nishiguchi, T. Matsumoto, H. Kanai, K. Utani, Y. Matsumura, W.-J. Shen, S. Imamura, Appl. Catal. A: Gen. 279 (2005) 273–277.
[32] R.S. Murthy, P. Patnaik, P. Sidheswaran, M. Jayamani, J. Catal. 109 (1988) 298–302.
[33] T. Nakajima, T. Yamaguchi, K. Tanabe, J. Chem. Soc., Chem. Commun. (1987) 394–395.
[34] T. Nakajima, K. Tanabe, T. Yamaguchi, I. Matsuzaki, S. Mishima, Appl. Catal. 52 (1989) 237–248.
[35] T.L. Barr, Y.L. Liu, J. Phys. Chem. Solids 50 (1989) 657–664.
[36] G.K. Padam, G.L. Malhotra, S.K. Gupta, Solar Energy Mater. 22 (1991) 303–318.
[37] A. Gurlo, M. Ivanovskaya, A. Pfau, U. Weimar, W. Göpel, Thin Solid Films 307 (1997) 288–293.
[38] B. Zhang, X. Tang, Y. Li, W. Cai, Y. Xu, W. Shen, Catal. Commun. 7 (2006) 367–372.